ELSEVIER

NeuroImage

www.elsevier.com/locate/ynimg
NeuroImage 34 (2007) 651–660

Nonlinearities in rapid event-related fMRI explained by stimulus scaling

Genevieve M. Heckman, Seth E. Bouvier, Valerie A. Carr, Erin M. Harley, Kristen S. Cardinal, and Stephen A. Engel*

UCLA Department of Psychology, Franz Hall 1282a, Los Angeles, CA 90095, USA

Received 15 June 2006; revised 30 August 2006; accepted 18 September 2006

Because of well-known nonlinearities in fMRI, responses measured with rapid event-related designs are smaller than responses measured with spaced designs. Surprisingly, no study to date has tested whether rapid designs also change the pattern of responses across different stimulus conditions. Here we report the results of such a test. We measured cortical responses to a flickering checkerboard at different contrasts using rapid and spaced event-related fMRI. The relative magnitude of responses across contrast conditions differed between rapid and spaced designs. Modeling the effect of the rapid design as a scaling of stimulus strength provided a good account of the data. The data were less well fit by a model that scaled the strength of responses. A similar stimulus scaling model has explained effects of neural adaptation, which suggests that adaptation may account for the observed difference between rapid and spaced designs. In a second experiment, we changed the stimulus in ways known to reduce neural adaptation and found much smaller differences between the two designs. Stimulus scaling provides a simple way to account for nonlinearities in event-related fMRI and relate data from rapid designs to data gathered using slower presentation rates.

Rapid event-related (ER) functional MRI is one of the most popular methods in cognitive neuroscience. In this method, individual stimuli or trials occur every few seconds or faster. Rapid ER fMRI has several advantages over traditional blocked designs, including the ability to randomize trial types and sort data based upon behavioral responses.

Yet, doubt lingers about the generality of results from experiments that use rapid ER fMRI. In particular, it is unclear whether results obtained with rapid event rates will replicate when events occur at slower rates. Almost every study that uses rapid ER designs assumes that fMRI responses show a certain kind of linearity. Specifically, they assume that responses in rapid designs can be predicted by simply adding appropriately placed responses measured in isolation to form the measured fMRI timecourse. Under this temporal superposition assumption, it is straightforward to estimate the average response for each event type, and this response will be identical to what the average response to that event type would be in a spaced design.

fMRI data, however, do not obey the assumption of temporal superposition. If superposition holds, then subtracting the response to an individual event from the response to a sequence of two events should yield a response that is identical in shape to the individual response. In actual fMRI data the subtracted response is smaller, often as little as 60–70% of the individual response (Dale and Buckner, 1997; Glover, 1999; Huettel and McCarthy, 2000, 2001; Boynton and Finney, 2003; Soon et al., 2003; Huettel et al., 2004a; Murray et al., 2006). Similar nonlinearities in response occur in sequences of blocks of events (Boynton et al., 1996; Robson et al., 1998; Vazquez and Noll, 1998; Glover, 1999; Ances et al., 2000b; Liu and Gao, 2000; Birn et al., 2001; Miller et al., 2001; Huettel et al., 2004b; Soltysik et al., 2004; Gu et al., 2005).

How damaging are these failures of superposition in practice? Most rapid ER studies at least implicitly assert that the failures are not critical, under the assumption that while rapid responses are smaller overall, the pattern of responses across conditions is the same as in spaced designs. A few studies have compared rapid to spaced ER designs at rates where superposition failures become most evident (Friston et al., 1998; Birn and Bandettini, 2005; Wager et al., 2005), but surprisingly no study has tested whether the relative magnitude of responses across conditions is preserved in rapid ER designs. That is, no study has examined whether the ratio of responses to two different conditions is equal in rapid and spaced ER fMRI.

Changes in the pattern of responses would be particularly damaging to quantitative fMRI applications, e.g., an attempt to correlate differences in fMRI response across conditions to differences in behavior across the same conditions. If the relative magnitudes of responses across conditions differed between rapid and spaced designs, then the correlation of these responses with behavioral measures could differ substantially.

There is good reason to believe that the pattern of responses will differ between the two design types. Because rapid designs drive neurons to higher response rates than spaced designs, they

* Corresponding author. Fax: +1 310 206 5895.
E-mail address: engel@psych.ucla.edu (S.A. Engel).
Available online on ScienceDirect (www.sciencedirect.com).

1053-8119/$ - see front matter © 2006 Elsevier Inc. All rights reserved.
doi:10.1016/j.neuroimage.2006.09.038

should increase neural adaptation. Such adaptation likely contributes to the overall reduction in response amplitudes observed in rapid designs (Boynton et al., 1996; Huettel and McCarthy, 2000; Birn et al., 2001; Buxton et al., 2004; Soltysik et al., 2004). Critically, neural adaptation in visual cortex does alter the pattern of responses across conditions (Sclar et al., 1989).

Here we test whether rapid and spaced ER designs yield the same pattern of responses across conditions. Formally, we capture this assumption with a *response scaling* model. The model predicts that rapid responses are copies of corresponding spaced responses scaled by a single constant factor.

We compare the response scaling model to a *stimulus scaling* model that predicts changes in the pattern of responses across conditions. The model is drawn from prior work on neural adaptation in visual cortex using both single unit electrophysiology and fMRI (Sclar et al., 1989; Gardner et al., 2005). The model predicts that rapid responses are copies of spaced responses to a set of stimuli whose strengths have been scaled by a single constant factor.

Experiment 1 measured the pattern of fMRI responses across multiple conditions using both rapid and spaced designs. We recorded blood oxygen level-dependent (BOLD) signals in visual cortex as subjects viewed checkerboards of different contrasts. The stimulus scaling model provided a better account of the data than the response scaling model.

Experiment 2 tested the hypothesis that neural adaptation caused the observed differences between spaced and rapid designs. We modified the stimuli from Experiment 1 in ways expected to decrease neural adaptation and observed smaller differences between the two types of designs.

Materials and methods

Subjects

Four subjects participated in each of three experiments (6 subjects total, 2 males and 4 females, ages 24–39, most participated in two or three of the experiments). All subjects were right-handed and had normal or corrected-to-normal vision. Procedures were approved by the UCLA Office for the Protection of Research Subjects.

Stimuli

Stimuli were presented to subjects using MR-compatible goggles (Resonance Technology, Inc.). The goggles were calibrated using a Photo Research PR-650 spectral radiometer. Independence of the red, green, and blue channels was tested, and the inverse gamma function for each channel was computed.

Pilot experiment

Subjects viewed radial checkerboard patterns (Fig. 1) that were presented for 500 ms and contrast reversed at a rate of 8 Hz. The checkerboard patterns had a radial frequency of 0.57 cycles per degree (cpd) of visual angle and an angular frequency of 18 cycles per stimulus (36 angular checks). The stimulus was centered on the display screen and subtended 21° of visual angle. Stimulus contrast was varied to obtain contrast response functions. Checkerboards in the pilot experiment were presented at 1, 10, and 100% contrast.

Experiment 1

Subjects viewed radial checkerboard patterns identical to those presented in the pilot experiment. To obtain contrast response functions, checkerboards were presented at 3, 6, 12, 24, 48, 72, and 96% contrast.

Experiment 2

Subjects viewed 1.0 cpd sinusoidal gratings that were presented for 116 ms. Stimulus contrast modulated over time following a Gaussian temporal envelope with a standard deviation of 29 ms. The gratings contrast reversed at a rate of 26 Hz, and their size and position on the display screen were identical to the checkerboard stimuli used in the pilot experiment and Experiment 1. These brief stimuli produced small fMRI responses, so we used three relatively high contrast levels to measure contrast response functions. Gratings were presented at 48, 72, and 96% contrast.

To reduce long-term neural adaptation, the phase (0, π/3, or 2π/3) and orientation (0, 45, 90, or 135°) of the gratings varied randomly across stimulus trials. The orientation order was constrained such that no stimulus trial had the same orientation as the stimulus trial preceding it.

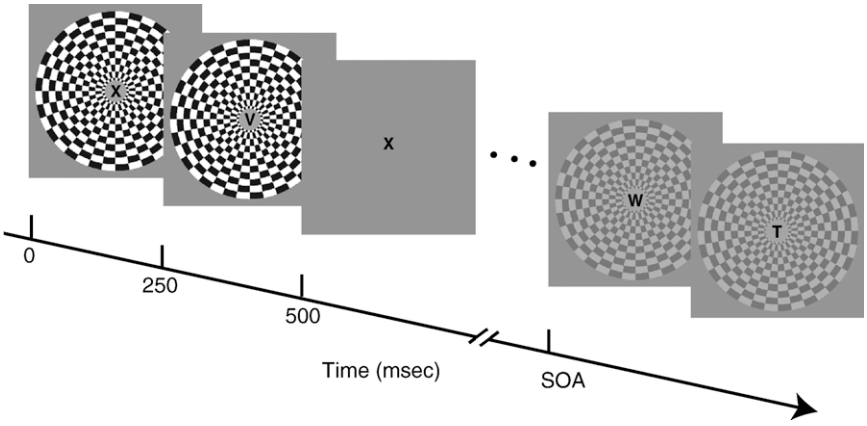

Fig. 1. Stimulus and methods. Subjects viewed contrast-reversing checkerboards (pilot and Experiment 1; Experiment 2 used gratings, not shown) that varied in their contrast and were presented for 500 ms with fixed temporal intervals between their onsets (SOA). To control attention, subjects monitored a string of letters for a target letter (see text for details).

Experimental design

Subjects in each experiment participated in an fMRI scanning session that included a single localizer scan followed by a series of experimental scans. In each scan, subjects performed a demanding letter recognition task at fixation while stimuli were presented in the surrounding visual field (Fig. 1).

Localizer scan

A block design localizer scan was used to identify cortical regions of interest (ROIs) that responded to the area of visual space where stimuli in the experimental scans were presented. High contrast radial checkerboard patterns, identical to those used in the pilot and Experiment 1, contrast reversed at 8 Hz (pilot and Experiment 1) and 10 Hz (Experiment 2) for 16 s, followed by 16 s of a uniform mean field. Eight of these stimulus cycles were presented.

Experimental scans

There were two types of event-related experimental scans, *spaced* and *rapid*, which differed in the length of time between stimulus presentations (called stimulus onset asynchrony, SOA). In the pilot experiment, spaced scans contained a 16-s SOA and rapid scans a 3-s SOA. In Experiments 1 and 2, spaced scans used a 3-s SOA and rapid scans a 1-s SOA.

In these scans, each event consisted of one stimulus presentation. Each scan contained several different types of events corresponding to the different stimulus contrasts presented in that experiment. Zero contrast events were also included as baseline (rest) trials. Each contrast condition occurred an equal number of times in each scan, and the order of contrast conditions within a scan was determined using *m*-sequences (Buracas and Boynton, 2002). Scans with 16, 3, and 1-s SOAs contained 24, 127, and 381 events, respectively. All scans were 384 s in length, and at least two repetitions of each type of scan (rapid and spaced) were performed.

Attention task

To control attention, subjects performed a demanding Rapid Serial Visual Presentation (RSVP) task at fixation throughout the duration of each experimental scan. Letters were presented one at a time in the center of the display screen, and subjects were instructed to press a button when they saw the letter "X" (Fig. 1). One of 14 possible letters was displayed every 250 ms, and the presentation order was pseudorandom with the constraint that no letter was presented twice in a row. Subjects in all experiments were able to perform the RSVP task, and performance did not differ between rapid and spaced scans (cross-experiment mean percent correct = 68.24 and 67.55, respectively; for each individual experiment all t values <1.6, all p values >0.17).

fMRI methods

Acquisition

Functional MRI data were collected using a Siemens Allegra 3 T scanner. During each scan, 12 slices of fMRI data, oriented perpendicular to the calcarine sulcus, were acquired each second using an echo-planar imaging sequence (TR = 1000 ms; TE = 45 ms; flip angle = 60°; voxel size = 3.1 × 3.1 × 4 mm; field of view = 200 mm). T2-weighted co-planar anatomical images were also acquired.

ROI definition

Visual areas V1, V2, V3, VP, V3a, and V4v were identified using reversals in phase-encoded polar angle retinotopy data (Engel et al., 1994; Sereno et al., 1995; DeYoe et al., 1996; Engel et al., 1997) acquired in a separate scanning session. MP-RAGE anatomical data for use in cortical flattening were also acquired in this session. Flattened cortical maps were generated using SurfRelax (Larsson, 2001) and retinotopic data were projected onto them using mrVista (http://white.stanford.edu/software). Regions of interest corresponding to known retinotopic areas were then drawn by hand by identifying the known reversals in polar angle retinotopy at their borders.

Data from the localizer and experimental scans were motion corrected and registered with the volume anatomical data using FSL FLIRT (Jenkinson et al., 2002), allowing the visual area ROIs to be projected onto the functional scan planes. Visual area ROIs were restricted to include only those voxels for which activity during the localizer scan was above a threshold correlation of 0.3 with a sinusoid at the on–off cycle frequency (see above). Changing this threshold did not change the overall pattern of results.

Data analysis

The fMRI time series from each active voxel was converted to a percent change score by subtracting and dividing by the mean of the voxel's time series across the scan. Time series were then averaged across voxels within each restricted visual area ROI. Linear estimates of fMRI response for each contrast condition within a scan were made using ordinary least squares. The design matrix contained one column for each time point in the response for each condition. fMRI responses were calculated for each scan and then averaged together within scan type, yielding one rapid and one spaced response for each contrast condition for each subject.

To combine data across subjects, subject average responses were normalized by dividing by the peak of the response to the highest contrast in the spaced SOA scans (in Experiment 1, responses were normalized to the second highest contrast because one subject ran only six of the seven contrast values). Normalized responses for each condition were then averaged across subjects. The height of each subject's normalized response at the time point of the peak in the group average was used as a measure of the fMRI response amplitude.

To test for effects of SOA and contrast, amplitudes were entered into three-way analyses of variance, with SOA, stimulus contrast, and subject as factors. To evaluate the fits of the models (see below), average peak response amplitudes for each SOA were plotted as a function of contrast condition to generate contrast response functions.

Models

We compared how well two models could account for the results of Experiments 1 and 2. A *response scaling* model predicts that rapid design responses are simply the spaced design responses multiplied by a single common scale factor. Such a scaling would correspond to a vertical shift of the contrast response function on a log–log axis (Fig. 2A). A *stimulus scaling* model predicts that rapid designs scale the effective strength (in this case, contrast) of the stimulus relative to that of spaced designs. In other words, the model predicts that rapid responses can be related to spaced responses by multiplying rapid contrast levels by a single common

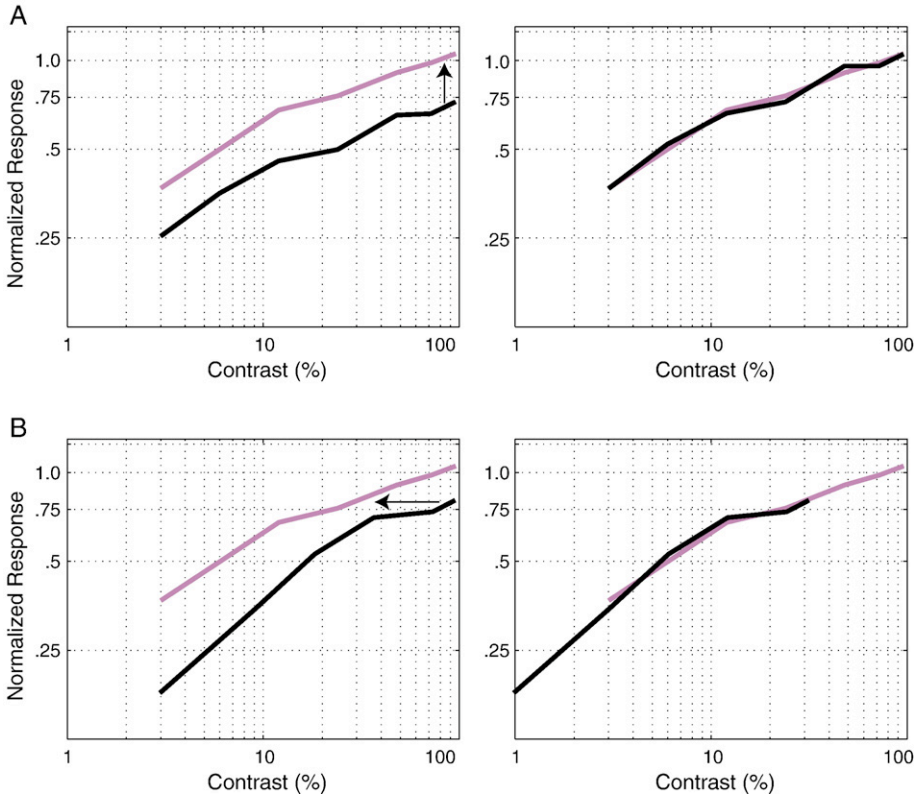

Fig. 2. Model Predictions. (A) *Response scaling model.* The left plot shows sample spaced data (taken from Experiment 1; pink curve) alongside hypothetical rapid data (black curve). The response scaling model predicts that shifting the rapid contrast response function along the vertical response axis will best align the two curves (right plot). (B) *Stimulus scaling model*. The left plot shows the same spaced data plotted alongside a second set of hypothetical rapid data (black curve). The stimulus scaling model predicts that shifting the rapid contrast response function along the horizontal contrast axis will best align the two curves (right plot).

scale factor. Such a scaling corresponds to a horizontal shift of the contrast response function on a log–log axis (Fig. 2B).

To formally define both models, we used a simple equation to parameterize fMRI response as a function of contrast:

$$R = Kc^n/(c^n + \sigma^n)$$

where R is the measured fMRI response, parameter c is stimulus contrast, n controls the steepness of the function, K scales the curve along the response axis and σ controls the position of the curve along the contrast axis. This equation has provided good accounts of neural contrast response functions measured with single unit electrophysiology (Sclar et al., 1989). In general, the model provided excellent fits to our fMRI contrast response functions. Importantly, our results do not depend upon this parameterization of the contrast response function. Any parameterization that adequately fit the data would give similar results.

The full response scaling model can be written as a pair of equations:

$$R_{\text{spaced}} = Kc^n/(c^n + \sigma^n)$$

and

$$R_{\text{rapid}} = s_{\text{resp}}Kc^n/(c^n + \sigma^n)$$

where s_{resp} is the scale factor relating the rapid to the spaced data. Because K controls the position of the curve along the response axis, the effect of the scale factor is to shift the rapid contrast response function along the vertical axis.

Similarly, the stimulus scaling model can be written as:

$$R_{\text{spaced}} = Kc^n/(c^n + \sigma^n)$$

and

$$R_{\text{rapid}} = K(s_{\text{stim}}c)^n/((s_{\text{stim}}c)^n + \sigma^n)$$

where s_{stim} is the scale factor relating the two types of data. The second equation here can equivalently be written as:

$$R_{\text{rapid}} = Kc^n/(c^n + (\sigma/s_{\text{stim}})^n)$$

Because σ controls the position of the curve along the contrast axis, this form of the equation shows that the scale factor shifts the contrast response function along the horizontal axis.

Model fitting

To determine which model could better account for our results, we fit both to our data. For each model, we found the parameters that best fit the rapid and spaced data simultaneously. Specifically, we minimized mean-squared error in predicting both contrast response functions using a nonlinear method (MATLAB fminsearch). We used the minimized mean-squared error as a measure of the quality of the model fit.

Plotting model fits

To illustrate the fit of the models graphically, we aligned the rapid and spaced contrast functions using the best-fitting scaling parameter from each model. For the response scaling model, the vertical distance between the two curves is estimated by s_{resp}. Accordingly, we divided the rapid response amplitudes by s_{resp} and plotted them with the unaltered spaced responses. This had the effect of shifting the rapid curve upward to align with the spaced curve. For the stimulus scaling model, the horizontal distance between the two curves is estimated by s_{stim}. Accordingly, we divided the rapid contrast levels by s_{stim} and used them to plot the rapid response amplitudes. This had the effect of shifting the rapid curve leftward to align with the spaced curve. For both models, we also plotted the predicted spaced responses interpolated across the entire contrast range.

Resampling analysis

To evaluate the reliability of model fitting results, we conducted resampling analyses. In each of 500 resamplings, we drew random samples of 4 subjects' data with replacement from our original data set. For each sample, we averaged across subjects to compute a new rapid and spaced contrast response function. We then fit the stimulus and response scaling models to this resampled function. For each resampling, we recorded the mean-squared error and parameter estimates for each model fit.

To compare models directly, we calculated the percentage of resamplings in which one model yielded lower mean-squared error than the other. We also computed confidence intervals on our parameter estimates by finding the range of parameters spanned by 95% of the resamplings.

Results

Pilot experiment

In a pilot experiment, a spaced ER design with a 16-s SOA and a rapid ER design with a 3-s SOA produced responses in V1 that did not differ significantly ($F(1,6)=1.79$; $p>0.2$). These results agree with prior studies that found only small differences between spaced designs and rapid designs with 4–5-s SOAs. Accordingly, in subsequent experiments we used the 3-s SOA as the spaced design and moved to a shorter, 1-s SOA for the rapid design.

Experiment 1

fMRI responses from V1 measured with a rapid, 1-s SOA were significantly smaller than responses measured with a spaced, 3-s SOA ($F(1,18)=52.2$; $p<0.01$). Fig. 3 plots the data, averaged across 4 subjects, as a function of stimulus contrast. Fig. 4A plots the peak amplitudes of the BOLD responses as a function of stimulus contrast (i.e., contrast response functions).

We next tested whether two simple models could account for the measured contrast response functions. Because the response scaling model accounts for the effects of rapid designs by multiplying the spaced fMRI responses by a constant factor, it predicts that the two curves will be shifted copies of each other along the log response axis. Thus an upward vertical shift of the rapid data should bring it into alignment with the spaced data (Fig. 2A).

Similarly, because the stimulus scaling model accounts for the effects of rapid designs by multiplying the strength of the stimuli by a constant factor, it predicts that the two curves will be shifted copies of each other along the log contrast axis. Thus a leftward shift of the rapid data should bring it into alignment with the spaced data (Fig. 2B).

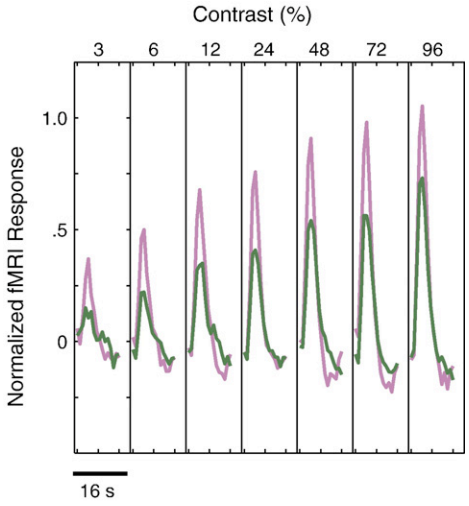

Fig. 3. Results of Experiment 1 in V1. Average normalized hemodynamic responses from spaced (3-s SOA, pink curve) and rapid (1-s SOA, green curve) designs. The black bar spans the size of the average standard error of the mean.

The stimulus scaling model fit the data from Experiment 1 better than the response scaling model. This can be easily seen by comparing the alignment of the two curves using the best fitting scale factors from each model (Figs. 4B and C; see Materials and methods for aligning procedure). The data fall closer together following a horizontal shift than a vertical shift.

Fig. 4 also shows the models' predicted responses for the spaced condition across the entire contrast range. The proximity of these predictions to the actual data demonstrates the ability of the models to fit the measured contrast response functions. In addition, both the spaced and the shifted rapid data fall closer to the predictions of the stimulus scaling model than the response scaling model.

The better fit of the stimulus scaling model was reliable. The mean-squared error of the best-fitting stimulus scaling model was lower than the mean-squared error for the best-fitting response scaling model in over 95% of samples in a resampling analysis (see Materials and methods).

The scaling parameter in the stimulus scaling model also provides a convenient way to quantify the effects of the rapid design. The rapid design scaled the effective contrast to 16% of the spaced design on average (median of resamplings), with the range 9%-27% covering 95% of the resamplings.

Experiment 2

The effects of the rapid ER design were greatly reduced in Experiment 2. Fig. 5 plots the average fMRI responses from V1 for the spaced and rapid scans. In contrast to Experiment 1, the rapid responses were only slightly smaller than the spaced responses and did not differ significantly from each other ($F(1,6)=0.08$; $p>0.5$).

We used the stimulus scaling model to compare quantitatively the effects of the rapid design in our two experiments. The median estimated stimulus scale factor was 97% in Experiment 2. Our resampling analysis showed that this number was reliably larger than the estimated scale factor in Experiment 1. In Experiment 2,

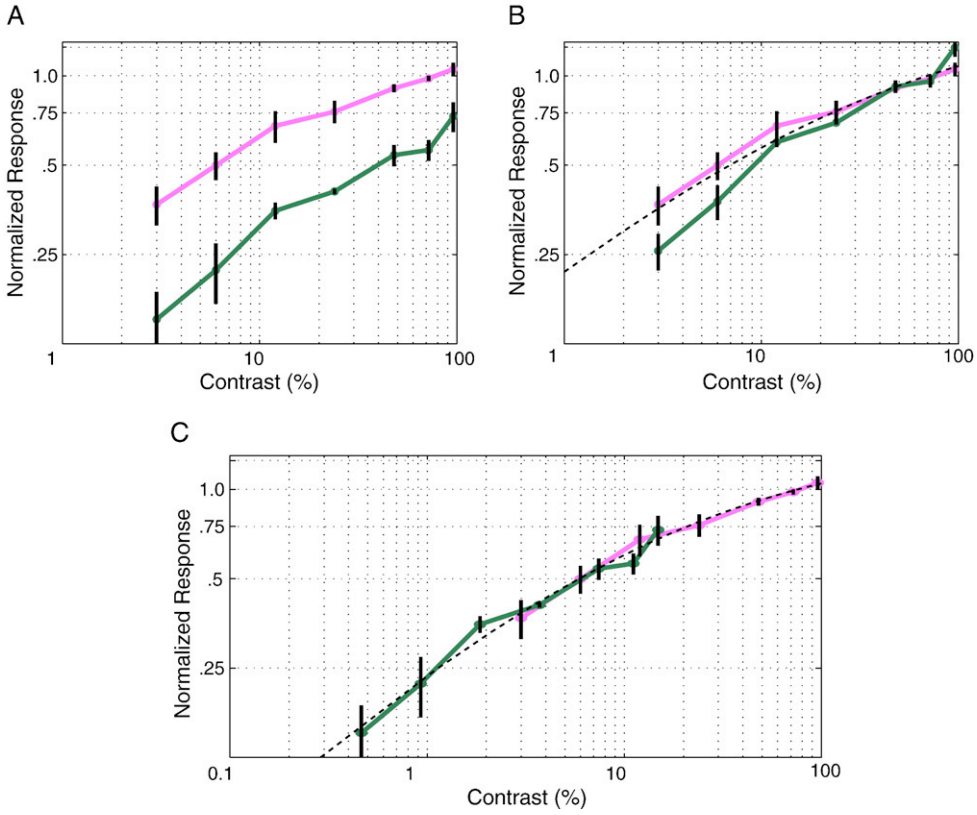

Fig. 4. Model fits to Experiment 1 data. (A) Peak fMRI spaced (pink) and rapid (green) responses as a function of stimulus contrast. The error bars span 2 standard errors of the mean. (B) Fit of the response scaling model. The rapid curve has been shifted vertically into optimal alignment with the spaced curve. The dotted black curve traces the model fit (see text for details). (C) Fit of the stimulus scaling model. The rapid curve has been shifted horizontally into optimal alignment with the spaced curve. The dotted black curve traces the model fit.

95% of resampled stimulus scale factors fell between 67% and 140%, which did not overlap with the confidence interval for Experiment 1 (9%–27%).

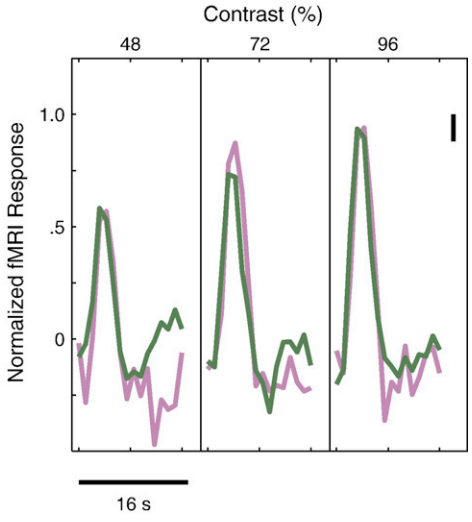

Fig. 5. Results of Experiment 2 in V1. (A) Average hemodynamic responses from spaced (3-s SOA, pink curve) and rapid (1-s SOA, green curve) designs. The black bar spans the size of the average standard error of the mean.

Extrastriate cortex

Compared to V1, results from extrastriate cortex showed larger differences between rapid and spaced designs. This was true for both Experiments 1 and 2. Fig. 6 plots contrast response functions from both experiments for areas V1, V2, VP, V3, V3a, and V4v, and Table 1 lists the estimated stimulus scaling parameters for each visual area. Prior studies have also found larger failures of linearity in visual areas beyond V1 (Huettel and McCarthy, 2001; Boynton and Finney, 2003).

Other results were generally similar in V1 and extrastriate cortex. The stimulus scaling model accounted for the results of Experiment 1 better than the response scaling model (percentage of resamplings where stimulus scaling fit better: V2: 87%, V3: 62%, VP: 91%, V3a: 54%, V4v: 84%). Also as in V1, the differences between rapid and spaced responses were an order of magnitude smaller in Experiment 2 than in Experiment 1. We were, however, unable to conduct the resampling analysis in Experiment 2 because the extrastriate data were relatively noisy. Specifically, many of the resampled contrast response functions were non-monotonic, which led to unacceptably poor model fits. Hence Table 1 reports scaling factors only from fits to the grand average data for Experiment 2.

Discussion

Our results suggest that rapid and spaced ER designs can be related in a relatively simple way: rapid designs scale the effective

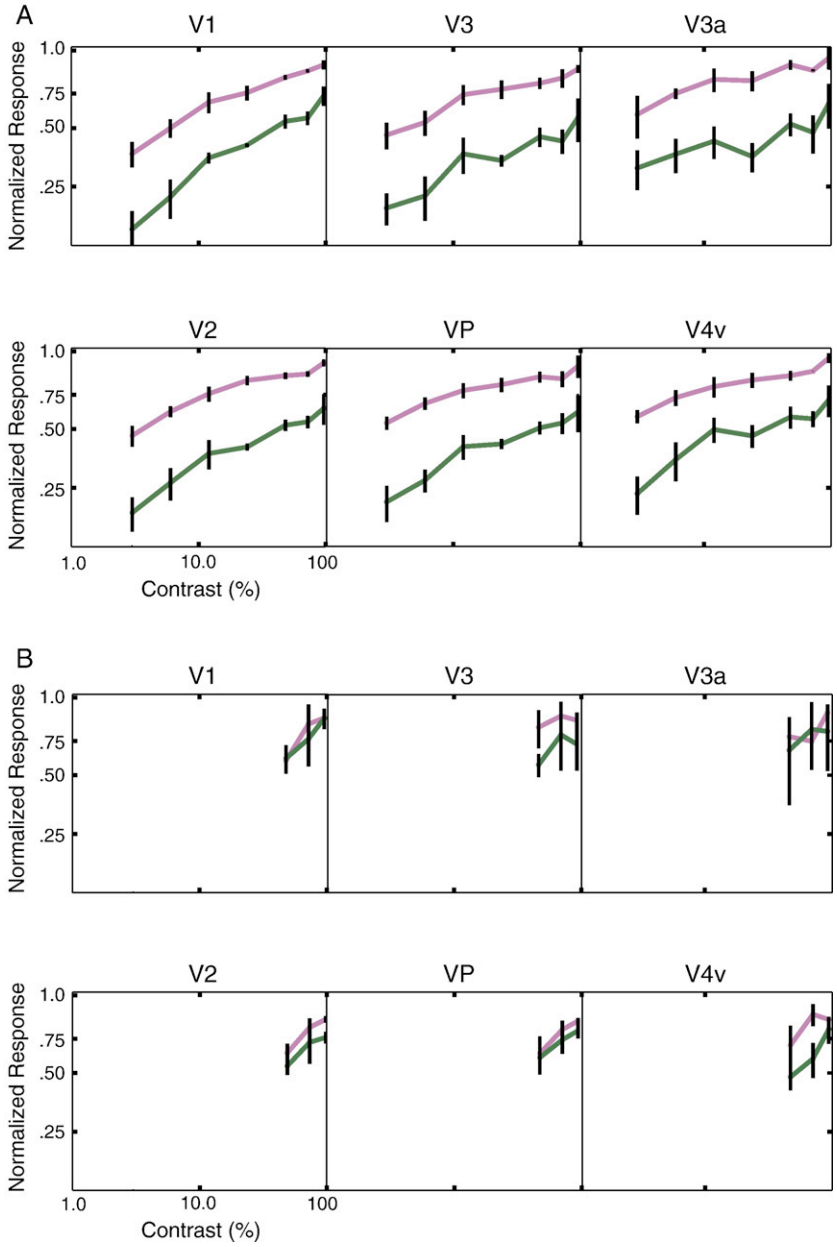

Fig. 6. Results of Experiment 1 (A) and Experiment 2 (B) for all visual areas. Average peak fMRI responses are plotted as a function of stimulus contrast. The error bars span 2 standard errors of the mean.

strength of stimuli to evoke hemodynamic responses. In V1, for example, the rapid design reduced the effective contrast of stimuli to 16% of their strength in the spaced design. This stimulus scaling model fit our data quite well and reliably better than a response scaling model.

The failure of the response scaling model means that the quantitative pattern of responses is not maintained across the change from rapid to spaced designs. Specifically, relative magnitudes of responses across conditions can differ between the two designs. In this important sense, data from rapid ER designs will not generalize to spaced designs. The stimulus scaling model, however, provides a simple way to account for these unintended effects of rapid ER designs.

A few prior experiments directly compared results from rapid and spaced designs (Friston et al., 1998; Pollmann et al., 1998; Miezin et al., 2000; Ollinger et al., 2001; Birn and Bandettini, 2005; Wager et al., 2005). Only one of these manipulated stimulus strength, and it used a 5-s SOA and found only very small differences between the rapid and spaced designs (Ollinger et al., 2001). Others have tested a single stimulus strength below 3-s ISIs and found that rapid designs produce substantially smaller responses than spaced designs (Friston et al., 1998; Birn and Bandettini, 2005; Wager et al., 2005). Our results support stimulus scaling as a simple quantitative account of these effects.

There remain two reasons for caution in interpreting our results. First, because brain regions differ in the neural and hemodynamic properties that produce failures of superposition (Birn et al., 2001; Huettel and McCarthy, 2001; Miller et al., 2001; Boynton and Finney, 2003; Huettel et al., 2004b; Soltysik et al., 2004), we cannot be certain how well the stimulus scaling model will account

Table 1
Results of Experiments 1 and 2

	Stimulus scaling factors					
	V1	V2	V3	VP	V3a	V4v
Exp 1	15% (8–27)	7% (3–13)	4% (1–16)	4% (2–8)	2% (0–9)	5% (2–13)
Exp 2	97%	70%	27%	82%	80%	58%

Each cell contains the stimulus scaling that best aligned the rapid and spaced contrast response functions. Ranges in parentheses contain 95% of scalings produced by 500 resamplings of the data.

for data in non-visual regions in the brain. Second, the failures of the response scaling model, while reliable, are small enough that it may still be adequate for some applications. This should be especially true when effects of neural adaptation are minimized.

Other simple models of the effects of rapid ER designs

Another model of the difference between rapid and spaced designs is a simple subtractive effect. This model predicts responses from rapid designs to be smaller than responses from spaced designs by a fixed absolute amount (as opposed to a fixed percentage). Simple subtractive models seem unlikely to explain differences between the two design types because they predict negative responses for conditions where spaced designs would yield small positive responses close to zero. Such inversions of weak responses do not appear in our data and have not been reported elsewhere in the literature. Nevertheless, we fit a simple subtractive model to our results and compared it to the stimulus scaling model. The stimulus scaling model fit our data better than the subtractive model, yielding a smaller mean-squared error in 96% of 500 resamplings of data from V1.

We cannot not rule out, however, models that combine several of the simple effects discussed above. To test models that, for example, combine subtractive and scaling effects, will require more powerful data.

Complex models of nonlinearities in rapid ER fMRI

A large number of prior studies have documented failures of temporal superposition in fMRI data (Boynton et al., 1996; Dale and Buckner, 1997; Robson et al., 1998; Vazquez and Noll, 1998; Glover, 1999; Ances et al., 2000b; Huettel and McCarthy, 2000; Liu and Gao, 2000; Birn et al., 2001; Huettel and McCarthy, 2001; Miller et al., 2001; Boynton and Finney, 2003; Soon et al., 2003; Huettel et al., 2004a,b; Soltysik et al., 2004; Gu et al., 2005; Murray et al., 2006). Other studies have found additional nonlinearities in fMRI; for example, when neural activity increases by a certain percentage, fMRI response fails to increase by the same percentage (e.g., Logothetis et al., 2001; Devor et al., 2003; Jones et al., 2004; Sheth et al., 2004; Hewson-Stoate et al., 2005; Wan et al., 2006).

Attempts to capture these nonlinearities in fMRI data have produced a number of complex models, including Volterra Kernels and biologically inspired models of neural and blood flow dynamics (Buxton and Frank, 1997; Friston et al., 1998, 2000; Miller et al., 2001; Buxton et al., 2004; Birn and Bandettini, 2005). Our results do not falsify these more complex models. Volterra kernels with enough terms can model any nonlinearity, and the biologically inspired models contain explicit parameters to capture neural adaptation, the likely cause of our effects. The complex models, however, may be difficult to use for many everyday fMRI applications. Fitting these models can be both computationally expensive and ambiguous if the data are not rich enough to constrain all their parameters.

The stimulus scaling model may represent a useful middle ground between assuming linearity and implementing the more complex nonlinear models (cf., Wager et al., 2005). For many applications, stimulus scaling may provide a relatively complete account of nonlinearities in the fMRI data that is easy to implement and interpret.

Sources of nonlinearities in fMRI

Two aspects of our results suggest that neural adaptation is a major source of nonlinearity in rapid ER designs. First, stimulus scaling effects, like those found in our fMRI data, have also been observed in electrophysiological studies of long-term adaptation. When individual neurons in visual cortex are driven strongly over a period of minutes, they reduce their responsiveness to subsequent stimuli. These long-term changes in responsiveness are well modeled as a scaling of effective stimulus contrast (Sclar et al., 1989). The similarity of this effect to the results of Experiment 1 suggests that neural adaptation may underlie the observed effects of rapid ER designs. Responses in the rapid design could be smaller than in the spaced design because the rapid stimulus presentation maintains high firing rates for a long period of time, causing neurons to reduce their responsiveness. A recent fMRI study also found effects of long-term adaptation that resemble stimulus scaling (Gardner et al., 2005).

Second, Experiment 2 reduced factors expected to produce neural adaptation and yielded much smaller differences between rapid and spaced designs. The stimuli were presented very briefly and were composed of sinusoidal gratings whose orientation changed from trial to trial. Such stimuli would be expected to generate lower average spiking rates in orientation selective V1 neurons and so should reduce adaptation. Prior work has long suggested that neural adaptation could be a major factor producing reductions in the BOLD response (Boynton et al., 1996; Huettel and McCarthy, 2000, Birn et al., 2001; Boynton and Finney, 2003; Buxton et al., 2004; Soltysik et al., 2004), and several fMRI studies have demonstrated long-term neural adaptation in human V1 (Tootell et al., 1998; Engel and Furmanski, 2001; Engel, 2005; Fang et al., 2005; Gardner et al., 2005; Larsson et al., 2006). Indeed, the assumption that adaptation influences the BOLD response has been used to develop novel experimental paradigms such as fMR adaptation (e.g., Grill-Spector and Malach, 2001).

Importantly, the results of Experiment 2 were not simply due to the stimuli producing smaller absolute fMRI responses overall. Responses in Experiment 2 were roughly equal in magnitude to responses for the lower contrast stimuli in Experiment 1. Yet, when we compared just these two sets of responses, we still observed much larger differences between rapid and spaced designs in Experiment 2.

We cannot rule out, however, that some part of the nonlinearity in rapid ER fMRI is due to non-neural factors, such as blood flow dynamics. A number of results are consistent with non-neural contributions to failures of superposition (Ances et al., 2000a; Miller et al., 2001; Pfeuffer et al., 2003; Martindale et al.,

2005; Murray et al., 2006). Nevertheless, in our paradigm, changing factors known to control neural adaptation greatly reduced nonlinearities in the BOLD response (see also Huettel et al., 2004a). This result has two possible interpretations. First, non-neural nonlinearities may be controlled by the same factors that control neural adaptation. Alternatively, these nonlinearities may only contribute weakly to signals in rapid ER fMRI. Resolving this issue will likely require further examination of temporal superposition with methods that combine imaging and electrophysiology.

Acknowledgments

The authors wish to thank Mark Cohen for helping with fMRI. For generous support of the UCLA Brain Mapping facility, the authors also wish to thank John Mazziotta, the Brain Mapping Medical Research Organization, Brain Mapping Support Foundation, Pierson-Lovelace Foundation, The Ahmanson Foundation, William M. and Linda R. Dietel Philanthropic Fund at the Northern Piedmont Community Foundation, Tamkin Foundation, Jennifer Jones-Simon Foundation, Capital Group Companies Charitable Foundation, Robson Family and Northstar Fund. The facility is supported by Grant Numbers RR12169, RR13642 and RR00865 from the National Center for Research Resources (NCRR), a component of the National Institutes of Health (NIH); the paper's contents are solely the responsibility of the authors and do not necessarily represent the official views of NCRR or NIH. This work was supported by NIH EY11862 to S.E., NSF graduate fellowship to G.H., and NIH MH015795.

References

Ances, B.M., Greenberg, J.H., Detre, J.A., 2000a. Effects of variations in interstimulus interval on activation-flow coupling response and somatosensory evoked potentials with forepaw stimulation in the rat. J. Cereb. Blood Flow Metab. 20, 290–297.

Ances, B.M., Zarahn, E., Greenberg, J.H., Detre, J.A., 2000b. Coupling of neural activation to blood flow in the somatosensory cortex of rats is time-intensity separable, but not linear. J. Cereb. Blood Flow Metab. 20, 921–930.

Birn, R.M., Bandettini, P.A., 2005. The effect of stimulus duty cycle and "off" duration on BOLD response linearity. NeuroImage 27, 70–82.

Birn, R.M., Saad, Z.S., Bandettini, P.A., 2001. Spatial heterogeneity of the nonlinear dynamics in the fMRI BOLD response. NeuroImage 14, 817–826.

Boynton, G.M., Finney, E.M., 2003. Orientation-specific adaptation in human visual cortex. J. Neurosci. 23, 8781–8787.

Boynton, G.M., Engel, S.A., Glover, G.H., Heeger, D.J., 1996. Linear systems analysis of functional magnetic resonance imaging in human V1. J. Neurosci. 16, 4207–4221.

Buracas, G.T., Boynton, G.M., 2002. Efficient design of event-related fMRI experiments using M-sequences. NeuroImage 16, 801–813.

Buxton, R.B., Frank, L.R., 1997. A model for the coupling between cerebral blood flow and oxygen metabolism during neural stimulation. J. Cereb. Blood Flow Metab. 17, 64–72.

Buxton, R.B., Uludag, K., Dubowitz, D.J., Liu, T.T., 2004. Modeling the hemodynamic response to brain activation. NeuroImage 23 (Suppl. 1), S220–S233.

Dale, A.M., Buckner, R.L., 1997. Selective averaging of rapidly presented individual trials using fMRI. Hum. Brain Mapp. 5, 329–340.

Devor, A., Dunn, A.K., Andermann, M.L., Ulbert, I., Boas, D.A., Dale, A.M., 2003. Coupling of total hemoglobin concentration, oxygenation, and neural activity in rat somatosensory cortex. Neuron 39, 353–359.

DeYoe, E.A., Carman, G.J., Bandettini, P., Glickman, S., Wieser, J., Cox, R., Miller, D., Neitz, J., 1996. Mapping striate and extrastriate visual areas in human cerebral cortex. Proc. Natl. Acad. Sci. U. S. A. 93, 2382–2386.

Engel, S.A., 2005. Adaptation of oriented and unoriented color-selective neurons in human visual areas. Neuron 45, 613–623.

Engel, S.A., Furmanski, C.S., 2001. Selective adaptation to color contrast in human primary visual cortex. J. Neurosci. 21, 3949–3954.

Engel, S.A., Rumelhart, D.E., Wandell, B.A., Lee, A.T., Glover, G.H., Chichilnisky, E.J., Shadlen, M.N., 1994. fMRI of human visual cortex. Nature 369, 525.

Engel, S., Glover, G., Wandell, B., 1997. Retinotopic organization in human visual cortex and the spatial precision of functional MRI. Cereb. Cortex 7, 181–192.

Fang, F., Murray, S.O., Kersten, D., He, S., 2005. Orientation-tuned fMRI adaptation in human visual cortex. J. Neurophysiol. 94, 4188–4195.

Friston, K.J., Josephs, O., Rees, G., Turner, R., 1998. Nonlinear event-related responses in fMRI. Magn. Reson. Med. 39, 41–52.

Friston, K.J., Mechelli, A., Turner, R., Price, C.J., 2000. Nonlinear responses in fMRI: the Balloon model, Volterra kernels, and other hemodynamics. NeuroImage 12, 466–477.

Gardner, J.L., Sun, P., Waggoner, R.A., Ueno, K., Tanaka, K., Cheng, K., 2005. Contrast adaptation and representation in human early visual cortex. Neuron 47, 607–620.

Glover, G.H., 1999. Deconvolution of impulse response in event-related BOLD fMRI. NeuroImage 9, 416–429.

Grill-Spector, K., Malach, R., 2001. fMR-adaptation: a tool for studying the functional properties of human cortical neurons. Acta Psychol. (Amst.) 107, 293–321.

Gu, H., Stein, E.A., Yang, Y., 2005. Nonlinear responses of cerebral blood volume, blood flow and blood oxygenation signals during visual stimulation. Magn. Reson Imaging 23, 921–928.

Hewson-Stoate, N., Jones, M., Martindale, J., Berwick, J., Mayhew, J., 2005. Further nonlinearities in neurovascular coupling in rodent barrel cortex. NeuroImage 24, 565–574.

Huettel, S.A., McCarthy, G., 2000. Evidence for a refractory period in the hemodynamic response to visual stimuli as measured by MRI. NeuroImage 11, 547–553.

Huettel, S.A., McCarthy, G., 2001. Regional differences in the refractory period of the hemodynamic response: an event-related fMRI study. NeuroImage 14, 967–976.

Huettel, S.A., Obembe, O.O., Song, A.W., Woldorff, M.G., 2004a. The BOLD fMRI refractory effect is specific to stimulus attributes: evidence from a visual motion paradigm. NeuroImage 23, 402–408.

Huettel, S.A., McKeown, M.J., Song, A.W., Hart, S., Spencer, D.D., Allison, T., McCarthy, G., 2004b. Linking hemodynamic and electrophysiological measures of brain activity: evidence from functional MRI and intracranial field potentials. Cereb. Cortex 14, 165–173.

Jenkinson, M., Bannister, P., Brady, M., Smith, S., 2002. Improved optimization for the robust and accurate linear registration and motion correction of brain images. NeuroImage 17, 825–841.

Jones, M., Hewson-Stoate, N., Martindale, J., Redgrave, P., Mayhew, J., 2004. Nonlinear coupling of neural activity and CBF in rodent barrel cortex. NeuroImage 22, 956–965.

Larsson, J., 2001. Imaging Vision: Functional Mapping of Intermediate Visual Processes in Man. Karolinska Institutet, Stockholm, Sweden.

Larsson, J., Landy, M.S., Heeger, D.J., 2006. Orientation-selective adaptation to first- and second-order patterns in human visual cortex. J. Neurophysiol. 95, 862–881.

Liu, H., Gao, J., 2000. An investigation of the impulse functions for the nonlinear BOLD response in functional MRI. Magn. Reson. Imaging 18, 931–938.

Logothetis, N.K., Pauls, J., Augath, M., Trinath, T., Oeltermann, A., 2001. Neurophysiological investigation of the basis of the fMRI signal. Nature 412, 150–157.

Martindale, J., Berwick, J., Martin, C., Kong, Y., Zheng, Y., Mayhew, J., 2005. Long duration stimuli and nonlinearities in the neural-haemodynamic coupling. J. Cereb. Blood Flow Metab. 25, 651–661.

Miezin, F.M., Maccotta, L., Ollinger, J.M., Petersen, S.E., Buckner, R.L., 2000. Characterizing the hemodynamic response: effects of presentation rate, sampling procedure, and the possibility of ordering brain activity based on relative timing. NeuroImage 11, 735–759.

Miller, K.L., Luh, W.M., Liu, T.T., Martinez, A., Obata, T., Wong, E.C., Frank, L.R., Buxton, R.B., 2001. Nonlinear temporal dynamics of the cerebral blood flow response. Hum. Brain Mapp. 13, 1–12.

Murray, S.O., Olman, C.A., Kersten, D., 2006. Spatially specific fMRI repetition effects in human visual cortex. J. Neurophysiol. 95, 2439–2445.

Ollinger, J.M., Shulman, G.L., Corbetta, M., 2001. Separating processes within a trial in event-related functional MRI. NeuroImage 13, 210–217.

Pfeuffer, J., McCullough, J.C., Van de Moortele, P.F., Ugurbil, K., Hu, X., 2003. Spatial dependence of the nonlinear BOLD response at short stimulus duration. NeuroImage 18, 990–1000.

Pollmann, S., Wiggins, C.J., Norris, D.G., von Cramon, D.Y., Schubert, T., 1998. Use of short intertrial intervals in single-trial experiments: a 3T fMRI-study. NeuroImage 8, 327–339.

Robson, M.D., Dorosz, J.L., Gore, J.C., 1998. Measurements of the temporal fMRI response of the human auditory cortex to trains of tones. NeuroImage 7, 185–198.

Sclar, G., Lennie, P., DePriest, D.D., 1989. Contrast adaptation in striate cortex of macaque. Vision Res. 29, 747–755.

Sereno, M.I., Dale, A.M., Reppas, J.B., Kwong, K.K., Belliveau, J.W., Brady, T.J., Rosen, B.R., Tootell, R.B., 1995. Borders of multiple visual areas in humans revealed by functional magnetic resonance imaging. Science 268, 889–893.

Sheth, S.A., Nemoto, M., Guiou, M., Walker, M., Pouratian, N., Toga, A.W., 2004. Linear and nonlinear relationships between neuronal activity, oxygen metabolism, and hemodynamic responses. Neuron 42, 347–355.

Soltysik, D.A., Peck, K.K., White, K.D., Crosson, B., Briggs, R.W., 2004. Comparison of hemodynamic response nonlinearity across primary cortical areas. NeuroImage 22, 1117–1127.

Soon, C.S., Venkatraman, V., Chee, M.W., 2003. Stimulus repetition and hemodynamic response refractoriness in event-related fMRI. Hum. Brain Mapp. 20, 1–12.

Tootell, R.B., Hadjikhani, N.K., Vanduffel, W., Liu, A.K., Mendola, J.D., Sereno, M.I., Dale, A.M., 1998. Functional analysis of primary visual cortex (V1) in humans. Proc. Natl. Acad Sci. U. S. A. 95, 811–817.

Vazquez, A.L., Noll, D.C., 1998. Nonlinear aspects of the BOLD response in functional MRI. NeuroImage 7, 108–118.

Wager, T.D., Vazquez, A., Hernandez, L., Noll, D.C., 2005. Accounting for nonlinear BOLD effects in fMRI: parameter estimates and a model for prediction in rapid event-related studies. NeuroImage 25, 206–218.

Wan, X., Riera, J., Iwata, K., Takahashi, M., Wakabayashi, T., Kawashima, R., 2006. The neural basis of the hemodynamic response nonlinearity in human primary visual cortex: Implications for neurovascular coupling mechanism. NeuroImage 32, 616–625.